Astringency assessment of persimmon by hyperspectral imaging

Sandra Munera[1](*), Cristina Besada[2](*), José Blasco[1], Sergio Cubero[1], Alejandra Salvador[2], Pau Talens[3], Nuria Aleixos[4](**)

[1)]Centro de Agroingeniería. Instituto Valenciano de Investigaciones Agrarias (IVIA). Ctra. Moncada-Náquera Km 4.5, 46113, Moncada, Valencia (Spain)

[2)]Centro de Tecnología Postcosecha. Instituto Valenciano de Investigaciones Agrarias (IVIA). Ctra. Moncada-Náquera Km 4.5, 46113, Moncada, Valencia (Spain)

[3)]Departamento de Tecnología de Alimentos. Universitat Politècnica de València. Camino de Vera, s/n, 46022 Valencia (Spain)

[4)]Departamento de Ingeniería Gráfica. Universitat Politècnica de València. Camino de Vera, s/n, 46022 Valencia (Spain)

* These authors contributed equally

**E-mail of the corresponding author: naleixos@dig.upv.es

ABSTRACT

One of the current challenges of persimmon postharvest research is the development of non-destructive methods that allow determination of the internal properties of the fruit, such as maturity, flesh firmness and astringency. This study evaluates the usefulness of hyperspectral imaging in the 460–1020 nm range as a non-destructive tool to achieve these aims in Persimmon cv. 'Rojo Brillante' which is an astringent cultivar. Fruit were harvested at three different stages of commercial maturity and exposed to different treatments of CO_2 (95% CO_2 – 20 ℃ – from 0 to 24 h) in order to obtain fruit with different levels of astringency. Partial Least Square (PLS) based methods were used to classify persimmon fruits by maturity and to predict flesh firmness from the average spectrum of each fruit. The results showed a 97.9% rate of correct maturity classification and an R^2_P of 0.80 for firmness prediction with only five selected wavelengths. For astringency assessment, as our results showed that the soluble tannins that remain after CO_2 treatments are distributed irregularly inside the flesh, a model based on PLS was built using the spectrum of every pixel in the fruit. The model obtained an R^2_P of 0.91 which allowed the creation of the predicted distribution maps of the tannins in the flesh of the fruit, thereby pointing to hyperspectral systems as a promising technology to assess the effectiveness of the

34 deastringency treatments that are usually applied before commercialising persimmons from

35 astringent cultivars.

36

37 *Keywords*: *Diospyros kaki*, fruit internal quality, soluble tannins, distribution map,

38 hyperspectral imaging, computer vision

39

40 **1. INTRODUCTION**

41 Astringency removal is required prior to commercialising astringent persimmon

42 cultivars. The astringency of persimmon fruit is due to the high soluble tannin content in

43 the flesh. Traditionally, the astringent cultivars have been consumed after fruit has been

44 submitted to an over-ripening treatment with exogenous ethylene; under these conditions

45 astringency removal is accompanied by a drastic loss of flesh firmness which hampers

46 postharvest handling of the fruit. For this reason, postharvest treatments which allow

47 astringency removal while preserving high flesh firmness have been developed in recent

48 years. Among them, the most widely used technique in commercial settings is based on

49 exposing fruits to high CO_2 concentrations (95% – 98%) for 24 h to 36 h. This method

50 promotes anaerobic respiration in the fruit, giving rise to an accumulation of acetaldehyde,

51 which reacts with the soluble tannins (ST). Tannins become insoluble at the end of the

52 treatment and astringency is no longer detected (Matsuo & Ito, 1982; Matsuo *et al.*, 1991).

53 The optimum duration of the CO_2 treatment depends on the cultivar but also on the stage

54 of fruit maturity (Besada *et al.*, 2010). If the treatment is too short, it may result in fruit

55 with residual astringency, and if extended excessively it may lead to losses of fruit quality

56 (Novillo *et al.*, 2014). Therefore, the optimum treatment conditions must be determined for

57 the different cultivars, but the stage of fruit maturity must also be taken into account.

58 Therefore, the knowledge of the fruit condition at harvest according to its stages of maturity

59 is a prerequisite to apply the adequate CO_2 treatment.

60 After application of the CO_2 treatment it is necessary to evaluate its effectiveness to

61 avoid residual astringency that could negatively affect the future buying intentions of

62 consumers. Currently, the effectiveness of deastringency treatment can be assessed by

63 measuring the content of ST that remain in the flesh, although this is a slow and destructive

64 analytical method, and thus commercially unfeasible. Another method to determine the

65 level of astringency of persimmon fruit is based on the reaction of ST (responsible for

66 astringency) with $FeCl_3$, which leads to a blue staining; the intensity of the staining

67 observed after a slice of the flesh is impregnated with $FeCl_3$ depends on its level of ST.

68 Although this method is faster and easier than the analytical determination of ST, it is also

69 destructive and subjective and therefore it is necessary to search for new rapid, reliable,

70 non-contact and non-destructive techniques.

71 Among them, computer vision represents a fast, accurate, and proved alternative for

72 monitoring fruit quality (Cubero *et al.*, 2011). However, this kind of sensors are limited to

73 analysing the external properties of the fruit like colour, size or the presence of external

74 defects, not being capable of detecting internal compounds like ST, responsible of the

75 astringency. Therefore, other methods capable of analyse internal compounds are

76 necessary. Spectroscopy is a non-destructive, inexpensive, rapid and reliable technique that

77 has traditionally been used in food chemistry for qualitative and quantitative determination

78 of different compounds in fruit samples, especially near infrared (NIR) spectroscopy

79 (Nicolaï *et al.*, 2007; Nicolaï *et al.*, 2014; Magwaza *et al.*, 2012; López *et al.*, 2013). This

80 technique has been utilised for the quantitative determination of soluble solids content

81 (SSC), firmness, acidity, dry matter, chemical substances such as glucose, sucrose, citric

82 acid, malic acid, starch or cellulose in different fruits (Schmilovitch *et al.*, 2000; Nagle *et*

83 *al.*, 2010; Theanjumpol *et al.*, 2013), and even to determine a maturity index (Jha *et al.*,

84 2013), internal quality index (Cortés *et al.*, 2016) or different appropriate indices for quality

85 analysis (Attila and János, 2011).

86 However, a major disadvantage of spectroscopy is that only can measure in a single point

87 of the sample. On the other hand, hyperspectral imaging is a non-destructive optical

88 technology that integrates the advantages of spectroscopy and conventional imaging to

89 obtain both spatial and spectral information simultaneously. It allows the visualisation of

90 internal compounds of the fruit distributed into the image which is not possible with

91 conventional spectroscopy (Gowen *et al.*, 2007; Lorente *et al.*, 2012) as in the case of the

92 ST of the persimmon, leading to a non-valid probe measurement and forcing to take

93 measurements in many places of the fruit surface (Noypitak *et al.*, 2015). Thus, using

94 hyperspectral imaging Mendoza *et al.*, (2011) developed a method for the in-line prediction

95 of firmness and SSC achieving coefficient of correlation between 0.83 and 0.95 for

96 prediction of firmness and between 0.67 and 0.87 for prediction of SSC in different apple

97 cultivars. Later they compared several spectral sensors to predict these properties (Mendoza

98 *et al.*, 2012). Cen *et al.* (2016) investigated the detection of internal chilling injuries in

99 pickling cucumbers using hyperspectral reflectance (500–675 nm) and transmittance (675–

100 1000 nm) achieving 100% of correct detection using SVM with the fruit travelling at 100

101 mm/s, which gives an idea of the potential of this technology for non-destructive in-line

102 quality control.

103   Ripeness has been one of the main features studied with this technology. Lleó *et al.*

104 (2011) used hyperspectral imaging (400–1000 nm) to predict the maturity of 'Rich lady'

105 peaches by computing different indices extracted from band ratios and combinations. The

106 application of these indices to create maps from the classification of individual pixels

107 showed that the ripening was not uniform throughout the entire fruit. Furthermore, the

108 ripening of intact bell peppers was studied by Schmilovitch *et al.* (2014) using

109 hyperspectral imaging (550–850 nm). They were able to relate some internal compounds

110 like SSC, total chlorophyll, carotenoid and ascorbic acid content with the spectral data by

111 means of a PLS regression, in all cases achieving an R^2 higher than 0.90 except for ascorbic

112 acid (0.72). The chemometric models they established were used to estimate internal

113 components in each pixel of the fruit image, thus allowing mapping of the quality

114 parameters in the intact peppers.

115   Apart from maturity, other properties can also be assessed. Yang *et al.* (2015) measured

116 anthocyanin content in lychee pericarp in the 350–1050 nm range. They created several

117 models achieving an R^2 of 0.92 using all wavelengths. The model was later applied to

118 entire fruits to create distribution maps with which to visualize the changes in anthocyanin

119 content during storage time. Liu *et al.* (2015) used multispectral images to predict lycopene

120 and phenolic compounds content in intact tomatoes. The comparison of methods based on

121 PLS, least squares-support vector machines (LS-SVM) and back propagation neural

122 networks (BPNN) showed BPNN to be the one that performed best, with an R^2 of 0.96. By

123 applying the model to each pixel of the tomato they were able to create prediction maps of

124 the intact tomatoes.

125   In persimmon fruit the use of this non-destructive technology to assess different quality

126 parameters is beginning to be studied. Hence, Wei *et al.* (2014) used hyperspectral imaging

127 to study the relationship between firmness and fruit maturity. Mohammadi *et al.* (2015)

128 also used image analysis techniques to evaluate the index of external colour of the fruits in

129 order to classify them into three stages of commercial maturity. Nevertheless, more studies

130 are necessary in this regard, particularly with fruit that will be commercialized with a firm

131 texture. Furthermore, to our knowledge, the potential of hyperspectral technology to detect

132 the level of astringency in persimmon has not been evaluated to date. Only some works

133 have been carried out to detect phenolic compounds related to astringency (Nogales-Bueno

134 *et al.*, 2014), focused especially on wine quality (Aleixandre-Tudó *et al.*, 2015; Boulet *et*

135 *al.*, 2016). And only one work has been found related to astringengy in persimmon using

136 NIR spectroscopy in the range of 660-960 nm (Noypitak *et al.*, 2015).

137   The aim of this work is to advance in the development of a non-destructive tool to assess

138 the astringency of persimmon fruits that have been gone under deastringency treatment,

139 since at present there are no methods or previous research focused on this aim for this type

140 of fruit, being still a demand from the industry.

141

142 **2. MATERIALS AND METHODS**

143 **2.1. Image acquisition and calibration**

144   The hyperspectral imaging system capable of acquiring images in the spectral range

145 400−1100 nm was composed of an industrial camera (CoolSNAP ES, Photometrics, AZ,

146 USA), and two liquid crystal tunable filters (LCTF) (Varispec VIS-07 and NIR-07,

147 Cambridge Research & Instrumentation, Inc., MA, USA) and a lens capable of covering the

148 whole spectral range without losing the focus (Xenoplan 1.4/23, Schneider Optics,

149 Hauppauge, NY, USA). The system was configured to capture images of 1392 x 1040

150 pixels with a spatial resolution of 0.14 mm/pixel and a spectral resolution of 10 nm. To

151 optimise the dynamic range of the camera, prevent saturated images and correct the spectral

152 sensitivity of the different elements of the system, a calibration of the integration time of

153 each band was performed by capturing the averaged reflectance of a white reference target

154 (Spectralon 99%, Labsphere, Inc, NH, USA) corresponding to 90% of the dynamic range of

155 the camera. The scene was illuminated by 12 halogen spotlights of 37 W each (Eurostar IR

156 Halogen MR16. Ushio America, Inc., CA, USA) powered by direct current (12 V), which

157 lit the scene indirectly by means of diffuse reflection inside a hemispherical dome where

158 whole fruits were introduced manually (Fig. 1). The inner surface of the aluminium dome

159 was painted in white and given a rough texture using a synthetic polish sprayer in order to

160 reduce directional reflections that could cause bright spots, thus providing highly

161 homogeneous light. A holder was used to place all samples at the same height inside the

162 dome.

163
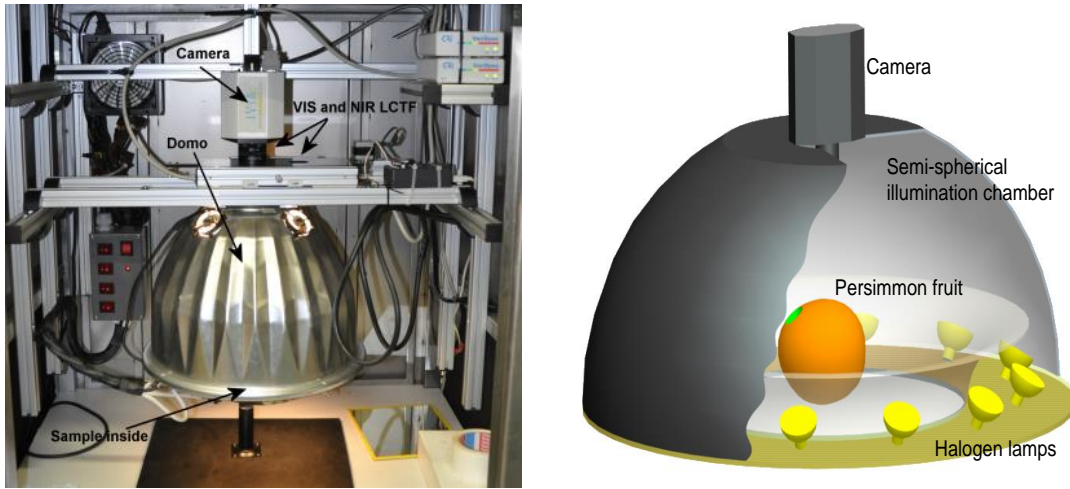
164 Figure 1. Configuration of the hyperspectral acquisition system

165

166 One hyperspectral image was captured of each fruit in reflectance mode in the working

167 spectral range 460–1020 nm, which together formed a database with a total of 150

168 hyperspectral images with 57 wavelengths each. Equation (1) (Gat, 2000) was used to

169 obtain the corrected relative reflectance of a pixel in the position *(x,y)* of the

170 monochromatic band λ.

171

$$\rho_{xy}(x, y, \lambda) = \frac{R^{abs}}{R^{abs}_{white}} = \rho^{Ref}(\lambda) \frac{R(x,y,\lambda) - R_{black}(x,y,\lambda)}{R_{white}(x,y,\lambda) - R_{black}(x,y,\lambda)} \qquad (1)$$

173

174 where $\rho^{Ref}(\lambda)$ is the standard reflectance of the white reference target (99% in this work),

175 *R(x,y,λ)* is the reflectance of the fruit captured by the charge-coupled device (CCD) sensor

176 of the camera, $R_{white}(x,y,\lambda)$ is the reflectance captured by the CCD of the white reference

177 target, and $R_{black}(x,y,\lambda)$ is the reflectance captured by the CCD while avoiding any light

178 source in order to quantify the electronic noise of the sensor.

179

2.2. Plant material and experimental design

Persimmon cv. 'Rojo Brillante' fruits were harvested in L'Alcudia (Valencia, Spain) at three different stages of commercial maturity (M1, M2 and M3) corresponding to early and late November, and mid-December. These three stages were intentionally selected in order to obtain fruit with different degree of maturity and therefore of firmness, since the success of the treatments depend on the fruit firmness at harvest (Salvador *et al.*, 2008) and therefore the possibility of assessing the astringency in fruits with different firmness was studied.

A total of 150 fruits with no skin damage and a homogeneous colour were selected and individually evaluated, corresponding to 50 fruits for each stage of maturity. In order to obtain different levels of astringency, fruits at each stage of maturity were divided into five homogeneous lots of 10 fruits each. Then the fruit was exposed to CO_2 treatments in closed containers (air containing 95% CO_2 at 20 ºC and 90% RH) for 0 h, 6 h, 12 h, 18 h and 24 h. Hyperspectral images of the intact fruits were acquired within 8 h after the CO_2 treatment. In addition, the physicochemical parameters (external colour, firmness, ST and astringency) to achieve the objectives of this study were evaluated individually in each fruit.

2.3. Physicochemical analysis

The external colour index (CI=1000*a*/*Lb*) was measured using a colorimeter (CR-300, Konica Minolta Inc, Tokyo, Japan) to know the colour of the fruits in each maturity stage at harvest. This index is based on the citrus colour index calculated using Hunter Lab colour values (Jiménez-Cuesta *et al*., 1981).

Flesh firmness was determined by means of a universal testing machine (4301, Instron Engineering Corp., MA, USA) equipped with an 8 mm puncture probe. The crosshead speed during testing was 1 mm/s. During the test, the force increased smoothly until it decreased drastically when the flesh was broken, and then the maximum peak force was registered. The results were expressed as the load (in N) required for breaking the flesh of the fruit on both sides after peel removal.

Analysis of variance (ANOVA) and Tukey´s test were conducted to determine significant differences during maturity (colour and firmness). For this purpose, the software Statgraphics (Manugistics Corp., Rockville, Md.) was used.

211

2.3.1 Assessment of firmness

212   **2.3.1 Assessment of firmness**

213   Among the physiological changes related to fruit maturation, such as colour or decline

214   of ST (Salvador *et al.*, 2007), the change in fruit firmness is one of the most important

215   feature to determine the optimum postharvest condition. In this regard, Salvador *et al.*

216   (2008) reported that fruit firmness can influence the effectiveness of the CO_2 treatment

217   because the loss of pulp structure associated to fruit softening may difficult the diffusion of

218   CO_2. To know if firmness could be predicted using the hyperspectral imaging system, a

219   representative ROI of the whole fruit surface was selected avoiding the stem and dark

220   borders (Fig. 2). The average spectrum of the pixels in the ROI was calculated and

221   considered as the fruit sample. Two thirds of the fruits in each maturity stage were used to

222   build the models and the remaining fruits were used as prediction set. A pre-processing

223   Standard Normal Variate (SNV) was applied to the spectra in order to remove scatter

224   effects from the original spectral data.

225
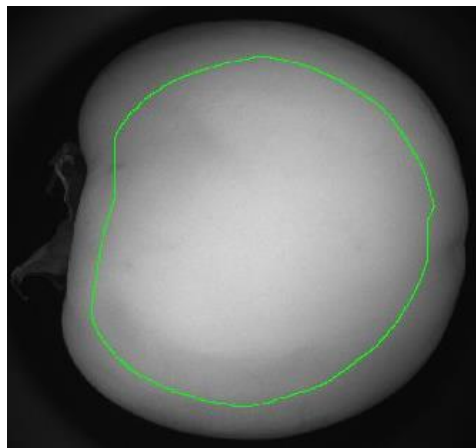
226
227   Figure 2. Hyperspectral image of a persimmon with the selected ROI (centred on 640 nm)
228

229   Hyperspectral systems are complex equipments that provide a huge amount of data. It is

230   therefore important to investigate whether the assessment of maturity can be performed

231   using a reduced number of selected wavelengths. The Successive Projections Algorithm

232   (SPA) has been proposed as a novel variable selection strategy for multivariate calibration

233   (Araújo *et al.*, 2001), and its purpose is to select wavelengths whose information content is

234   minimally redundant. The SPA is a forward selection method that builds an ordered chain

235 of *k* variables where each element is selected in order to present the least collinearity with

236 the previous ones. The collinearity between variables is assessed by the correlation between

237 the respective column vectors of the calibration matrix. As it is an iterative method, this

238 means that several subsets containing up to *k* variables can be formed. Finally, in order to

239 choose the most appropriate subset, Multiple Linear Regression models are built to

240 compare them in the terms of the RMSE. In order to select the most important bands, SPA

241 was applied using MATLAB R2015a (The MathWorks, Inc. MA, USA) on the calibration

242 set of fruits.

243   PLS-discriminant analysis (PLS-DA) was applied in order to know if it was possible to

244 separate the fruit into the three stages of maturity at harvest using both, the entire spectrum

245 and only the variables selected by the SPA. In a similar way, PLS regression (PLS-R) was

246 used to predict the firmness including the data provided by the universal testing machine

247 instead of the stages of maturity. A single 10-fold cross-validation was used to choose the

248 optimal number of LV and accuracy and predictive capability of the PLS-R models were

249 evaluated by RMSE and coefficient of determination R^2. The software used in this study

250 was The Unscrambler X 10.1 (CAMO Software, Oslo, Norway).

251

252 **2.3.2 Assessment of Astringency**

253   The level of astringency of each individual fruit was determined in three different ways:

254   1) Each fruit was cut in half and pressed against 10x10 cm filter paper soaked in a 5%

255       $FeCl_3$ solution, obtaining a blue print whose quantity and intensity gave information

256   about the ST content and its distribution. This process is an alternative technique to

257   the Folin-Denis method used in industry to determine the level of astringency in

258   fruit batches, and it has only been used to show visually the internal distribution of

259   the ST and its intensity.

260   2) A flesh sample from each fruit was frozen at −20 ℃ and later the content of ST was

261   analysed using the Folin-Denis method (Taira, 1995). The results were expressed as

262   relative ST in fresh weight, being the quantitative reference used in our analyses.

263   3) The level of astringency of the fruit was evaluated by a sensory panel consisting of

264   10 semi-trained staff members of IVIA familiar with persimmon fruit and

265   astringency attribute. Astringency was determined using a 5-point scale from 1-
266   non-astringent or absence of astringency to 5-intensely astringent.

267

268   To assess the astringency using the hyperspectral imaging system a new approach
269   was used. As the current method used in the industry is based on the printing of the
270   content and distribution of ST, the imaging system was used also to create maps of the
271   distribution of the ST. Hence, the individual spectrum of each pixel in the image was
272   used to predict the astringency of that pixel, thus using the spectral but also the spatial
273   information provided by an image-based technology. A PLS model was built using 12
274   persimmons from the whole set of fruits. Six fruits (two of each maturity stage) were
275   selected from the non-treated fruit, and thus considering as very astringent and another
276   six (two of each maturity stage) from the batch that were treated for 24 h.

277   A total of 67456 pixels labelled as astringent or non-astringent were selected from
278   the aforementioned fruits. The spectra of these pixels were used to build the PLS model
279   that was internally validated by means of a 10-fold cross-validation. The model was
280   then projected to the rest of the fruit to obtain maps of the distribution of the
281   astringency in the fruits.

282

283 **3. RESULTS AND DISCUSSION**

284 **3.1. Assessment of firmness**

285   The colour index and the firmness of the samples at harvest are shown in Table 1. It is
286 observed that the firmness value decreases as the fruit ripen, but in all cases studied having
287 high firmness. In the case of the colour, the values measured indicate that fruit was
288 changing from orange to red, as the increasing of the CI is due to an increase of the *a* value
289 and a reduction of *b,* both variables expressed in Hunter Lab values.

290

291   Table 1. Colour index and firmness values for the three stages of maturity at harvest

	M1	M2	M3
CI	9.46 ± 1.77 [a]	18.20 ± 3.32 [b]	21.6 ± 4.05 [c]
Firmness (N)	43.85 ± 4.1 [a]	30.8 ± 3.5 [b]	24.4 ± 4.9 [c]

The SPA used to reduce the dimensionality achieved an optimal set of five wavelengths (570, 590, 680, 710, 990 nm). These wavelengths are associated to the range of absorption bands of carotenoids (570 and 590 nm) (Choudhary *et al.*, 2009; Merzlyak *et al.*, 2003), chlorophyll (680 and 710 nm) (Lleó *et al.*, 2011; Rajkumar *et al.*, 2012) and water content (990 nm) (Lu and Peng, 2006).

Table 2 shows the results obtained for the classification of persimmon fruits in terms of their stage of maturity. Both models, using all and the optimal wavelengths, achieved high percentage of fruits classified correctly (>90%). As regarding the classification of each maturity stage, fruits of M2 were worst classified in both models.

Table 2. Maturity classification (%) of the test set by PLS-DA using all and selected wavelengths

	#LV	Class	M1	M2	M3	Correct classification
All wavelengths	4	M1	94.6	0.9	0.0	93.9
		M2	4.0	91.5	4.4	
		M3	1.4	7.6	95.6	
Selected wavelengths	2	M1	92.9	2.7	0.0	90.0
		M2	4.9	86.3	9.1	
		M3	2.2	11.0	90.9	

Table 3 shows the results of the flesh firmness prediction, obtaining similar results using all and the selected wavelengths. Values obtained were 0.77 and 0.80 for R^2 of the prediction using all and selected wavelengths, respectively. The results were not as good as the prediction results of Wei *et al.* (2014), who achieved an R^2 value of 0.91, but they worked with non-treated fruit having higher firmness differences between the harvest and the marketing. In the case of 'Rojo Brillante' persimmon, if they are sold as firm fruit after receiving some treatment to remove astringency, values below 10 N are considered as unsuitable from a commercial point of view (Salvador *et al.*, 2004).

Table 3. Results of firmness prediction using PLS-R with all and selected wavelengths

	#LV	R^2_{CV}	$RMSE_{CV}$	R^2_P	$RMSE_P$
All wavelengths	2	0.80	4.34	0.77	3.89
Selected wavelengths	2	0.80	4.34	0.80	3.66

As stated, firmness is highly related to maturity, but also to astringency. As softening progresses further, acetaldehyde produced at rather low levels in the flesh also may promote tannin polymerization. Thus, in extremely soft fruit, both tannin-pectin complex formation and acetaldehyde-tannin polymerization may be involved in the reduction of astringency (Taira *et al.*, 1997). Then, it is very important for this fruit to demonstrate that deastringency treatments do not affect the firmness.

3.2. Astringency assessment

The application of the different CO_2 treatments resulted in fruit with a wide range of ST contents across the three stages of maturity studied, being the content of ST after different treatments between 0.75% and 0.03% (Fig. 3). This was supported by the sensory evaluation of the fruit (data not shown) that revealed that an ST content of 0.03% was related to non-astringent fruit, which is in agreement with Salvador *et al.*, (2007) and Besada *et al.*, (2010). ST contents higher than 0.4% led to intensely astringent fruit (sensory value of 5), while values between 0.04% and 0.4% were evaluated by the panellist as slight to medium astringency.

The evaluation of the ST by the $FeCl_3$ method revealed a progressive reduction of the ST in the fruit as the duration treatment was longer. Moreover, it was observed that the reduction of the ST advanced from the calyx area. Figure 3 shows examples of different blue prints obtained for the different duration of the CO_2 treatments.
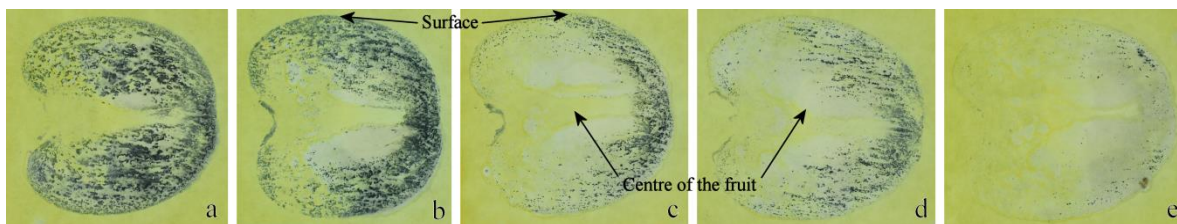
342   Figure 3. Astringency distribution from the blue print (FeCl$_3$) for persimmons CO$_2$ treated

343   during different hours: a) non-treated; b-e) treated with CO$_2$ for 6 h, 12 h, 18 h and 24 h

344

345   The model built from astringent and non-astringent pixels using PLS was used to predict

346   the astringency of the pixels of the validation fruits and to visually compare them with the

347   prints obtained using the destructive FeCl$_3$ method. Figure 4 shows several examples of the

348   predicted distribution map of the astringency of randomly chosen persimmons that were

349   treated with CO$_2$ for different periods to achieve different levels of astringency (from

350   untreated fruit that was evaluated by the panellist as intensely astringent to 24 h-treated

351   fruit, in which astringency was not detected, including medium or slight astringency for

352   fruit treated for 6 h, 12 h or 18 h). A colour scale was used, being non-astringent pixels

353   represented by the blue colour and astringents by red colour.

354

355
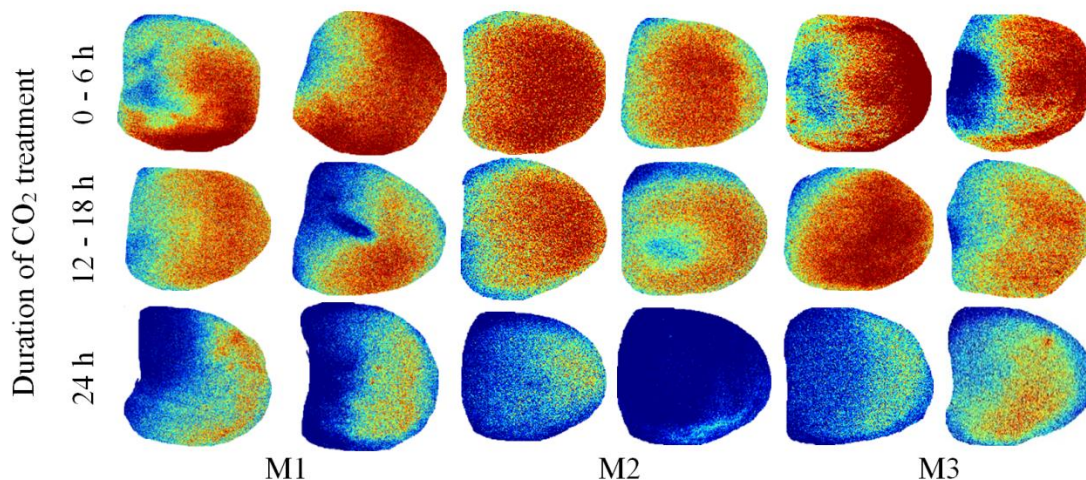
Figure 4. Samples of prediction maps from hyperspectral images of persimmons in the three maturity stages

Prediction maps obtained using hyperspectral imaging system showed astringency distribution on the surface of each fruit. It was observed that the distribution of astringency in fruits under different treatments followed a very similar pattern to one obtained using destructive methods based on $FeCl_3$ prints (Fig. 3). In Figure 4, it is clearly visible that fruits with no treatment (0 h) or very short (6 h) treatment had the highest astringency while models predicted lower astringency for fruits receiving treatment for 24 h. In addition, it was evident in all the images that most astringency concentrated at the bottom of the fruit, while began to be removed from the calyx area, following the same trend shown in Fig. 3.

This work contributes to lay the basis for future non-destructive tools capable to decide whether a persimmon is or not astringent in postharvest or contains residual astringency after a defective treatment, thus ensuring high quality fruit to consumers. Despite the penetration depth of the hyperspectral imaging that can be of few millimetres in the fruit, the blue prints showed that the tannins are distributed similarly in the internal part of the fruit and near the surface, and therefore can be captured by the hyperspectral images. Hence, hyperspectral imaging can be considered a valuable technique for the non-destructive evaluation of the astringency and a potential alternative to current destructive methods.

377   Results achieved coincide with those achieved by Noypitak *et al*. (2015). They carried

378   out a study for astringency by using spectrometry in the near-infrared zone (700–1050 nm)

379   and measured in twelve different parts of the fruit, later calculating the average of all the

380   measurements and obtaining results of around R^2 of 0.95. However, the authors worked

381   with very astringent persimmons and persimmons in which all astringency was completely

382   eliminated, avoiding the intermediate levels of astringency. Moreover, at a difference from

383   this study, the authors used plastic bags to remove the astringency of the fruits, thereby

384   causing a sharp loss of firmness that could have large influence the results.

385

386   **4. CONCLUSIONS**

387   The results of the present study showed VIS/NIR hyperspectral imaging to be a

388   promising non-destructive tool to assess the astringency of persimmon fruits that have been

389   gone under deastringency treatment. On one hand, the SPA method was used to select a

390   small set of wavelengths (570, 590, 680, 710, 990 nm) that allowed fruit classification

391   according to their stage of maturity using PLS-DA. The success rate obtained using the

392   entire spectrum was slightly higher than using only the five selected wavelengths, but in

393   both cases higher than 90%. In addition, an optimum prediction of the flesh firmness was

394   achieved using PLS regression. Moreover, using the selected wavelengths, the coefficient

395   of determination R^2_P was higher (0.80) than using the full spectrum (0.77).

396   On the other hand, it was built a predictive model that, applied to fruit submitted to

397   deastringency treatments, allowed to create maps of the distribution of the ST that were

398   compared visually with the traditional and subjective method based in the blue prints, to

399   differentiate non-astringent fruits from those completely or medium astringent, thus

400   creating a comprehensive non-destructive tool that can be used as alternative to the current

401   destructive method based on $FeCl_3$ prints. Therefore, hyperspectral imaging should be

402   considered as a potential non-destructive method to evaluate the effectiveness of the

403   deastringency treatments.

404

405   **ACKNOWLEDGEMENTS**

412

REFERENCES

414 Aleixandre-Tudó, J.L., Nieuwoudt, H. & Du Toit, W.J. (2015). Robust ultraviolet-visible
415   (UV-Vis) partial least squares (PLS) model for tannin quantification in red wine. Journal
416   of Agricultural and Food Chemistry 63, 1088–1098.

417 Araújo, M. C. U., Saldanha, T. C. B., Galvão, R. K. H., Yoneyama, T., Chame, H. C. &
418   Visani, V. (2001). The successive projections algorithm for variable selection in
419   spectroscopic multicomponent analysis. Chemometrics and Intelligent Laboratory
420   Systems, 57(2), 65–73.

421 Attila, N. & János, T. (2011). Sweet cherry fruit analysis with reflectance measurements.
422   Journal Analele Universității din Oradea, Fascicula: Protecția Mediului, 17, 263-270.

423 Besada, C., Salvador, A., Arnal, L. & Martínez-Jávega, J.M., (2010). Optimization of the
424   duration of deastringency treatment depending on persimmon maturity. Acta
425   Horticulturae 858, 69–74.

426 Boulet, J.C., Trarieux, C., Souquet, J.M., Ducasse, M.A., Caillé, S., Samson, A., Williams,
427   P., Doco, T. & Cheynier, V. (2016). Models based on ultraviolet spectroscopy,
428   polyphenols, oligosaccharides and polysaccharides for prediction of wine astringency.
429   Food Chemistry 190, 357–363.

430 Cen, H., Lu, R., Zhu, Q. & Mendoza, F. (2014). Nondestructive detection of chilling injury
431   in cucumber fruit using hyperspectral imaging with feature selection and supervised
432   classification. Postharvest Biology and Technology 111, 352–361.

433 Choudhary, R., Bowser, T. J., Weckler, P., Maness, N. O. & McGlynn, W. (2009). Rapid
434   estimation of lycopene concentration in watermelon and tomato puree by fiber optic
435   visible reflectance spectroscopy. Postharvest Biology and Technology 52, 103–109.

436 Cortés, V., Ortiz, C., Aleixos, N., Blasco, J., Cubero, S. & Talens, P. (2016). A new
437   internal quality index for mango and its prediction by external visible and near-infrared
438   reflection spectroscopy. Postharvest Biology and Technology, 118, 148-158.

439 Cozzolino, D., Kwiatkowski, M.J., Parker, M., Cynkar, W.U., Dambergs, R.G., Gishen, M.
440   & Herderich, M.J. (2004). Prediction of phenolic compounds in red wine fermentations
441   by visible and near infrared spectroscopy. Analytica Chimica Acta 513, 73–80.

442 Cubero, S., Aleixos, N., Moltó, E., Gómez-Sanchis, J. & Blasco, J. (2011). Advances in
443   machine vision applications for automatic inspection and quality evaluation of fruits and
444   vegetables. Food Bioprocess Technology 4, 487–504.

445 Food Chemistry 173, 482–488

446 Gat, N. (2000). Imaging spectroscopy using tunable filters: A review. Technical report,
447   Opto-Knowledge Systems Inc. OKSI.

448 Gómez-Sanchis, J., Blasco, J., Soria-Olivas, E., Lorente, D., Escandell-Montero, P.,
449   Martínez-Martínez, J.M., Martínez-Sober, M. & Aleixos, N., (2013). Hyperspectral
450   LCTF-based system for classification of decay in mandarins caused by Penicillium
451   digitatum and Penicillium italicum using the most relevant bands and non-linear
452   classifiers. Postharvest Biology and Technology 82, 76-86.

453 Gowen, A. A., O'Donnell, C. P., Cullen, P. J., Downey, G., & Frias, J. M. 2007.
454   Hyperspectral imaging—an emerging process analytical tool for food quality and safety
455   control. Trends in Food Science and Technology 18, 590–598.

456 Jha, S.N., Jaiswal P, Narsaiah K, Sharma R, Bhardwaj R, Gupta M, Kumar R. (2013).
457   Authentication of mango varieties using near infrared spectroscopy. Agricultural
458   Research, 2(3):229 – 235. 3.

459 Jiménez-Cuesta MJ, Cuquerella J, Martínez-Jávega JM. (1981) Determination of a color
460   index for citrus fruit degreening. In Proceedings of the International Society of
461   Citriculture, Vol. 2, 750-753.

462 Liu, C., Liu, W., Chen, W., Yang, J. & Zheng, L. (2015). Feasibility in multispectral
463   imaging for predicting the content of bioactive compounds in intact tomato fruit. Food
464   Chemistry 173, 482-488.

465 Lleó, L., Roger, J.M., Herrero-Langreo, A., Diezma-Iglesias, B. & Barreiro, P. (2011).
466   Comparison of multispectral indexes extracted from hyperspectral images for the
467   assessment of fruit ripening. Journal of Food Engineering 104, 612–620.

468 Lopez, A., Arazuri, S., Garcia, I., Mangado, J., Jaren, C. (2013) A review of the application
469   of near-infrared spectroscopy for the analysis of potatoes. J. Agric. Food Chem., 61,
470   5413–5424.

471 Lorente, D., Aleixos, N., Gómez-Sanchis, J., Cubero, S., García-Navarrete, O.L. & Blasco,
472   J., (2012). Recent advances and applications of hyperspectral imaging for fruit and
473   vegetable quality assessment. Food Bioprocess Technology 5, 1121–1142.

474 Lu, R. & Peng, Y., (2006). Hyperspectral Imaging for assessing peach fruit firmness.
475   Biosystems Engineering 93, 161–171.

476 Magwaza, L.S., Opara, U.L., Nieuwoudt, H., Cronje, P.J.R., Saeys, W. & Nicolaï, B.
477   (2012) NIR Spectroscopy Applications for Internal and External Quality Analysis of
478   Citrus Fruit-A Review. Food and Bioprocess Technology 5, 425-444

479 Matsuo, T. & Ito, S. (1982). A model experiment for de-astringency of persimmon fruit
480   with high carbon dioxide: in vitro gelation of kaki-tannin by reacting with acetaldehyde.
481   Journal of Agricultural Food Chemistry 46, 683–689.

482 Matsuo, T., Ito, S. & Ben-Arie, R. (1991). A model experiment for elucidating the
483   mechanism of astringency removal in persimmon fruit using respiration inhibitors.
484   Journal of the Japanese Society for Horticultural Science 60, 437–442.

485 Mendoza, F., Lu, R., Ariana, D., Cen, H. & Bailey B. (2011). Integrated spectral and image
486   analysis of hyperspectral scattering data for prediction of apple fruit firmness and
487   soluble solids content. Postharvest Biology and Technology 62, 149-160.

488 Mendoza, F., Lu, R. & Cen, H. (2012). Comparison and fusion of four nondestructive
489   sensors for predicting apple fruit firmness and soluble solids content. Postharvest
490   Biology and Technology 73, 89–98.

491 Merzlyak, M.N., Solovchenko, A.E. & Gitelson, A.A. (2003). Reflectance spectral features
492   and non-destructive estimation of chlorophyll, carotenoid and anthocyanin content in
493   apple fruit. Postharvest Biology and Technology 27, 197–211.

494   Mohammadi, V., Kheiralipour, K. & Ghasemi-Varnamkhasti, M. (2015). Detecting
495   maturity of persimmon fruit based on image processing technique. Scientia Horticulturae
496   184, 123–128.

497   Nagle, M., Mahayothee, B., Rungpichayapichet, P., Janjai, S. & Müller, J. (2010). Effect of
498   irrigation on near-infrared (NIR) based prediction of mango maturity. Scientia
499   Horticulturae, 125(4), 771-774.

500   Nicolaï, B.M., Beullens, K., Bobelyn, E., Peirs, A., Saeys, W., Theron, K.I. & Lammertyn,
501   J. (2007). Non-destructive measurement of fruit and vegetable quality by means of NIR
502   spectroscopy: A review. Postharvest Biology and Technology, 46 (2), 99–118.

503   Nogales-Bueno, J., Hernández-Hierro, J.M. & Heredia. F.J. (2014). Determination of
504   technological maturity of grapes and total phenolic compounds of grape skins in red and
505   white cultivars during ripening by near infrared hyperspectral image: a preliminary
506   approach. Food Chemistry 152, 586–591.

507   Novillo, P., Salvador, A., Llorca, E., Hernando, I. & Besada, C. (2014). Effect of CO2
508   deastringency treatment on flesh disorders induced by mechanical damage in
509   persimmon. Biochemical and microstructural studies. Food Chemistry 145, 453 – 463.

510   Noypitak, S., Terdwongworakul, A., Krisanapook, K. & Kasemsumran, S. (2015).
511   Evaluation of astringency and tannin content in 'Xichu' persimmons using near infrared
512   spectroscopy. International Journal of Food Properties, 18:1014–1028.

513   Salvador, A., Arnal, L., Besada, C., Larrea, V., Quiles, A. & Pérez-Munuera, I. (2007).
514   Physiological and structural changes during ripening and deastringency treatment of
515   persimmon cv. 'Rojo Brillante'. Postharvest Biology and Technology 46, 181–188.

516   Salvador, A., Arnal, L., Besada, C., Larrea, V., Quiles, A. & Pérez-Munuera, I. (2008).
517   Reduced effectiveness of the treatment for removing astringency in persimmon fruit
518   when stored at 15 ºC. Physiological and microstructural study. Postharvest Biology and
519   Technology 49, 340 – 347.

520   Salvador, A., Arnal, L., Carot, J.M.., Carvalho, C.P.. & Jabaloyesm, J.M. (2006). Influence
521   of different factor son firmness and color evolution during the storage of persimmon cv.
522   'Rojo Brillante'. Sensory and Nutritive Qualities of Food, 71(2), 170–175.

523   Salvador, A., Arnal, L., Monterde, A. & Cuquerella, J. (2004). Reduction of chilling injury
524   symptoms in persimmon fruit cv 'Rojo brillante' by 1-MCP. Postharvest Biology and
525   Technology 33, 285–291.

526   Schmilovitch, Z., Ignat, T., Alchanatis, V., Gatker, J., Ostrovsky, V. & Felföldi, J. (2014).
527   Hyperspectral imaging of intact bell peppers. Biosystems engineering Special Issue:
528   Image Analysis in Agriculture 117, 83-93.

529   Schmilovitch, Z., Mizrach, A., Hoffman, A., Egozi, H. & Fuchs, Y. (2000). Determination
530   of mango physiological indices by near-infrared spectrometry. Postharvest Biology and
531   Technology, 19(3), 245-252.

532   Taira, S. (1995). Astringency in persimmon. In: Linskens, H.F., Jackson, J.F. Fruit
533   Analysis. Springer, Hannover, Germany, pp. 97–110.

534   Taira, S., Ono, M. & Matsumoto N. (1997) Reduction of persimmon astringency by
535   complex formation between pectin and tannins. Postharvest Biology and Technology 12,
536   265–271

537   Theanjumpol, P., Self, G., Rittiron, R., Pankasemsu, T., & Sardsud, V. (2013). Selecting
538   Variables for Near Infrared Spectroscopy (NIRS) Evaluation of Mango Fruit Quality.
539   Journal of Agricultural Science, 5(7).

540   Vélez-Rivera, N., Blasco, J., Chanona-Pérez, J., Calderón-Domínguez, G., Perea-Flores,
541   M.J., Arzate-Vázquez, I., Cubero, S. & Farrera-Rebollo, T. (2014). Computer vision
542   system applied to classification of "Manila" mangoes during ripening process. Food and
543   Bioprocess Technology 7, 1183-1194.

544   Wei, X., Liu, F., Qiu, Z., Shao, Y. & He, Y. (2014). Ripeness Classification of Astringent
545   Persimmon Using Hyperspectral Imaging Technique. Food and Bioprocess Technology
546   7, 1371–1380.

547   Yahaya, O.K.M., MatJafri, M.Z., Aziz, A.A. & Omar, A.F. (2015). Visible spectroscopy
548   calibration transfer model in determining pH of Sala mangoes. Journal of
549   Instrumentation, 10, T05002.

550   Yang, Y.C., Sun, D.-W. Pu, H., Wang, N.N. & Zhu, Z. (2015). Rapid detection of
551   anthocyanin content in lychee pericarp during storage using hyperspectral imaging
552   coupled with model fusion. Postharvest Biology and Technology 103, 55–65.

553